

Supporting Information

Thioether-functionalized Covalent Triazine Nanospheres: A Robust Adsorbent for Mercury Removal

Sujan Mondal^a, Sauvik Chatterjee^a, Saptarsi Mondal^b and Asim Bhaumik^{*,a}

^aSchool of Materials Science, Indian Association for the Cultivation of Science, Jadavpur, Kolkata-700032, India

^bSchool of Chemical Sciences, Indian Association for the Cultivation of Science, Jadavpur, Kolkata-700032, India

Methodology

The repetitive unit of the ligand has been optimized for a different number of Hg²⁺ ions using Gaussian 16 suites of the program.¹ We have employed B3LYP density functional for the convenient result and in many cases, it has been used previously to illustrate weak and strong non-covalent interactions.²⁻⁷ For C, H, N and S we have used 6-31+G(d,p) basis function whereas we have applied LanL2DZ basis function and effective core potential for the heavy Hg²⁺ which found to produce a reliable result in earlier studies. During optimization we have employed the frozen core approximation and tight convergence criterion. Harmonic frequency calculations have been performed to ensure that all the structures are local minimum structures. The stabilization energy for all the complexes have been calculated based on the following equation

$$\Delta E_{Stab} = E_{Comp} - E_{Hg^{2+}} - E_{Lig} \quad (0.1)$$

Where, E_{Comp} , $E_{Hg^{2+}}$, and E_{Lig} are zero-point vibrational energy (ZPVE) corrected energies of the complex, the Hg^{2+} , and the ligand. To understand the nature of a different kind of non-covalent interaction, we have generated molecular density map using Atoms in Molecules (AIM) software and performed AIM analysis.⁸⁻¹⁷ Further, we have calculated the electron density (ρ) and Laplacian of electron density ($\nabla^2 \rho$, L) at each bond critical points (BCPs) to know the nature of the interaction between two interacting atoms. It is important to mention that only those BCPs have been considered whose ρ and L is higher than 0.002 and 0.02 a.u., respectively, as they confirm the existence of non-covalent interaction from earlier studies. To measure the strength of any interaction we have calculated the ellipticity of the interaction (ε) at the bond critical point (BCP) using the following equation

$$\varepsilon = \frac{\lambda_1}{\lambda_2} - 1 \quad (0.2)$$

Where, λ 's are the negative vectors associated with the hessian of ρ at that CP and $\lambda_2 \leq \lambda_1$.

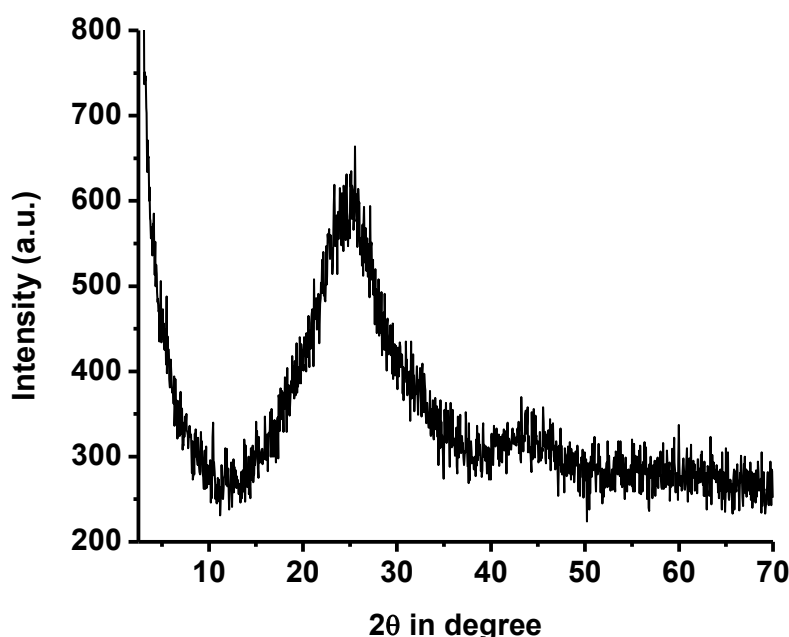


Figure S1. Powder x-ray diffraction pattern of SCTN-1 material.

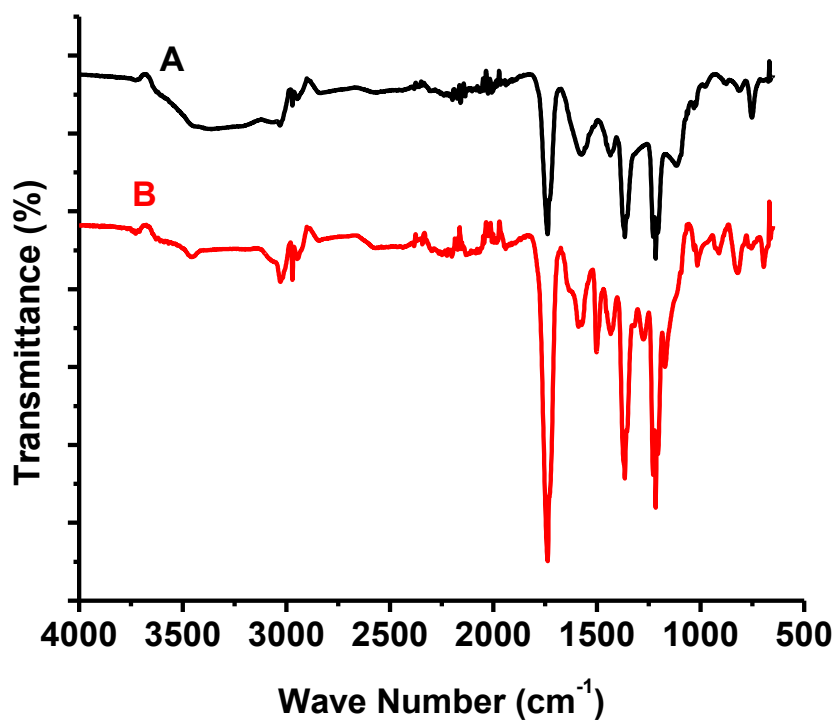


Figure S2. IR spectrum of SCTN-1 (A) and post-adsorbed SCTN-1 material (B).

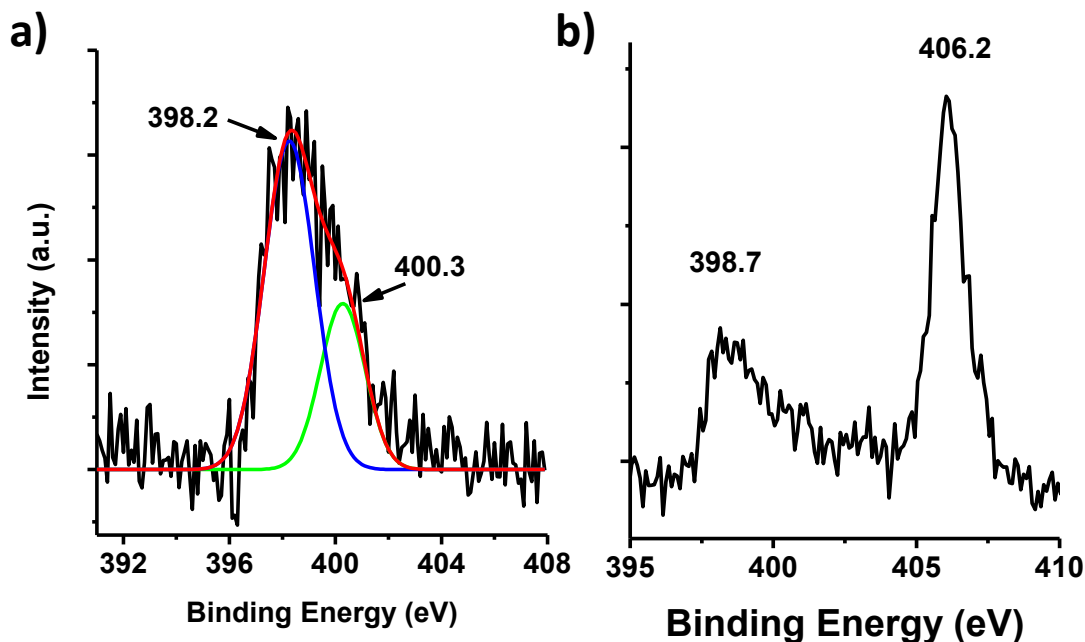


Figure S3. N1s XPS spectrum of before (a) and after mercury adsorbed (b) SCTN-1. The additional peak appeared in post adsorbed SCTN-1 at 406.2 eV indicates the presence of NO_3^- which comes from the solution prepared for adsorption studies.

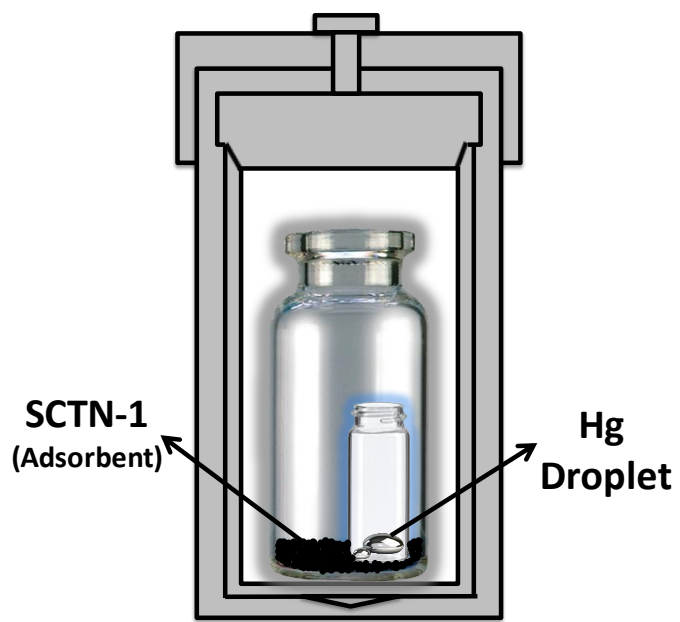


Figure S4. Schematic diagram of mercury [Hg(0)] vapor capture experiment.

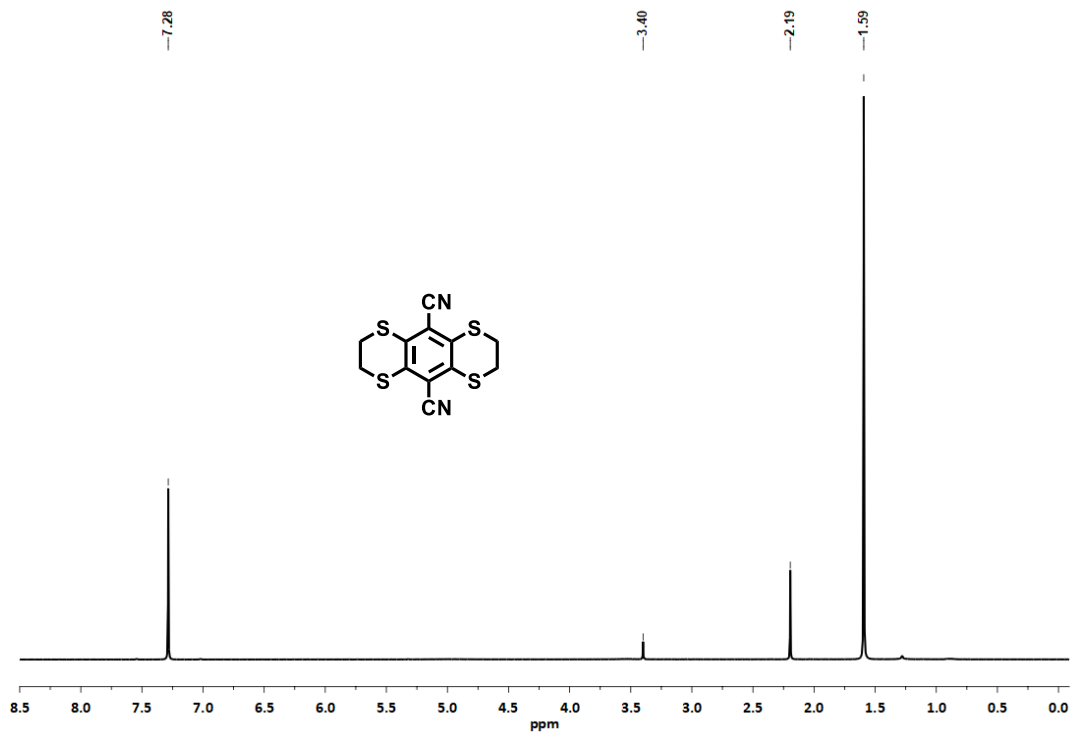


Figure S5. ¹H NMR of thio-ether based igand (1).

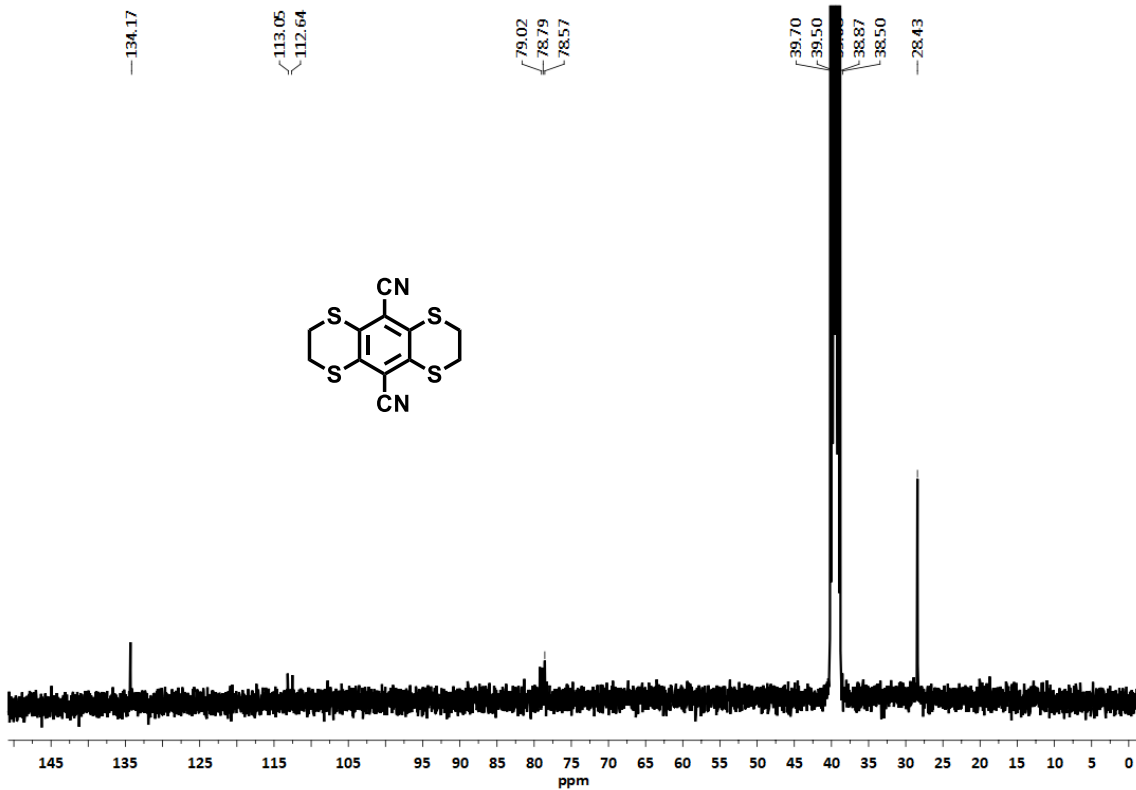


Figure S6. ¹³C NMR of thio-ether based ligand (1).

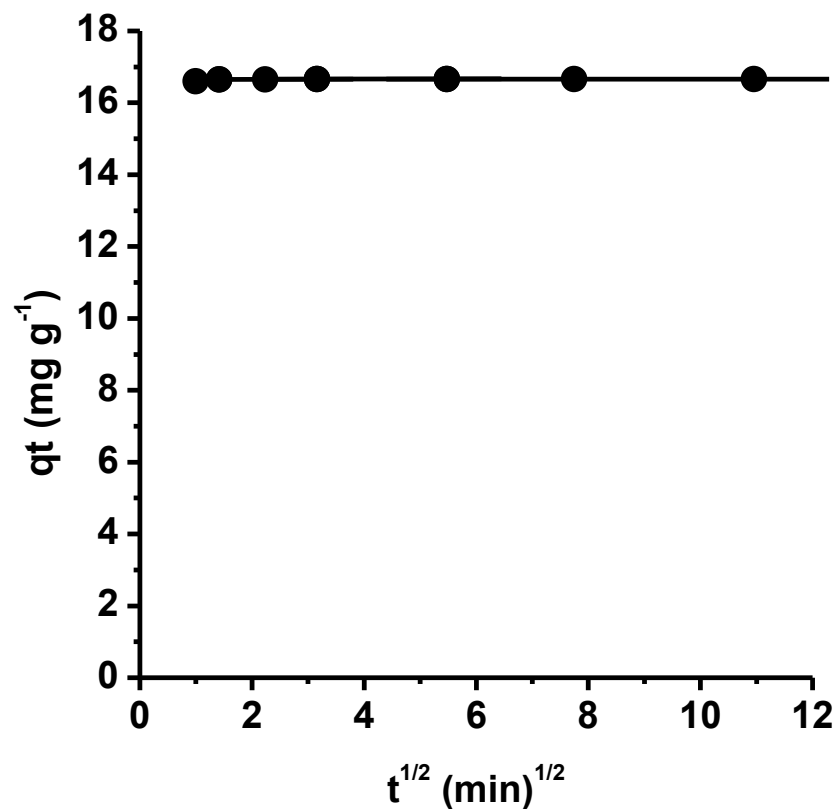


Figure S7. Kinetics of mercury adsorption according to the interparticle diffusion model.

Table S1: List of stabilization energy (ΔE_{Stab} , kcal/mole) of different complexes between Hg^{2+} and the ligand calculated at B3LYP/6-31+G(d,p);LanL2DZ(Hg) level of theory.

System	ΔE_{Stab} (kcal/mole)	ΔE_{Stab}^{ZPVE} (kcal/mole)	Comment
COMP11	-213.9	-213.6	Very stable
COMP12	-194.7	-195.7	Very stable
COMP13	+48.6	+45.7	Unstable
COMP14	+504.1	+498.2	Unstable

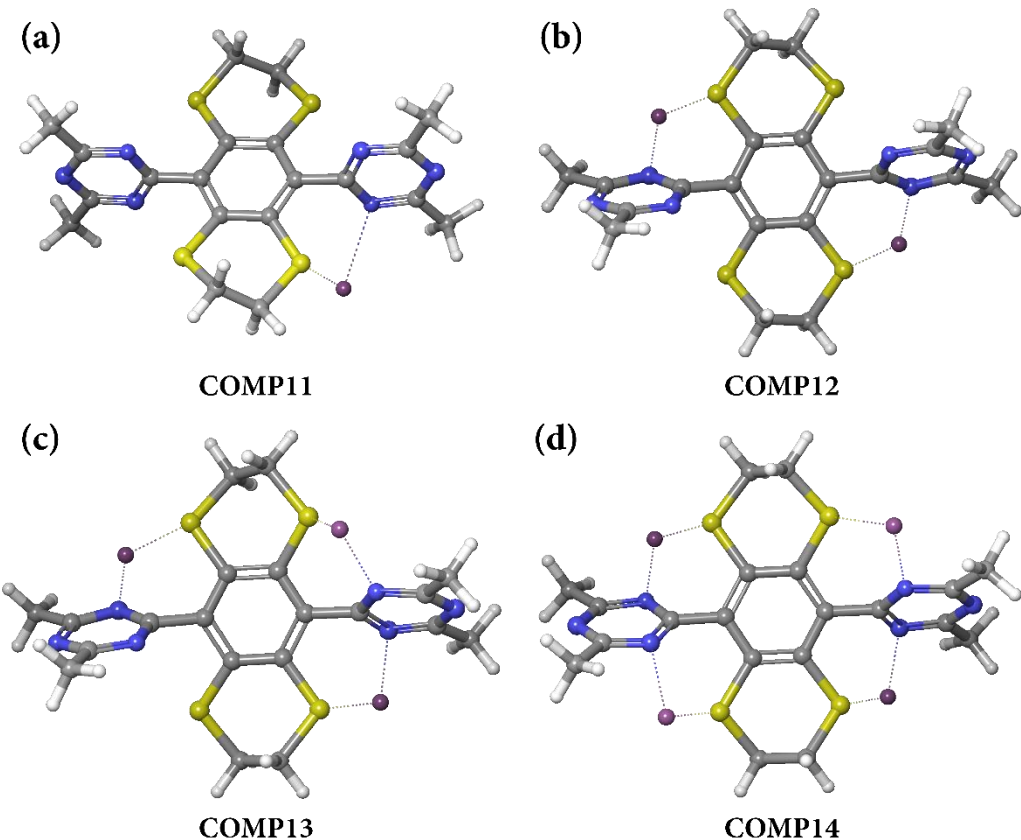


Figure S8. Optimized geometry of the complex between Hg^{2+} and the ligand, (a) COMP11 (1:1), (b) (a) COMP12 (1:2), (c) COMP13 (1:3), and (d) COMP14 (1:4) calculated at B3LYP/6-31+G(d,p);LanL2DZ(Hg) level of theory using Gaussian 16, Rev. A03 suites of program. The spheres in white, yellow, grey, blue and violet color are H, S, C, N, and Hg respectively.

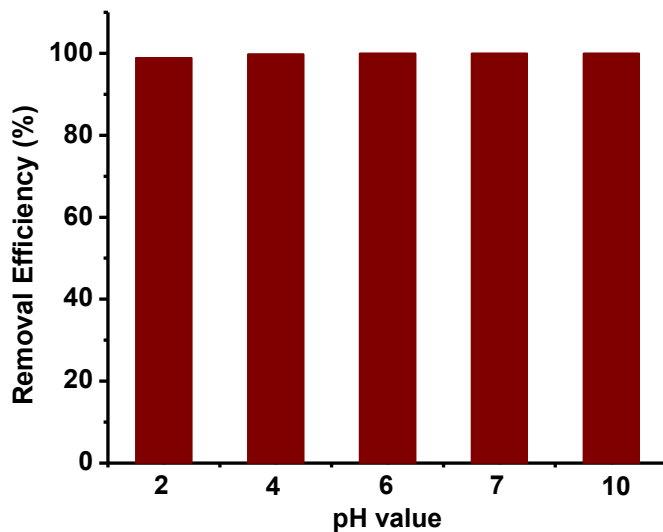


Figure S9. Removal of Hg(II) under different pH conditions after 2h.

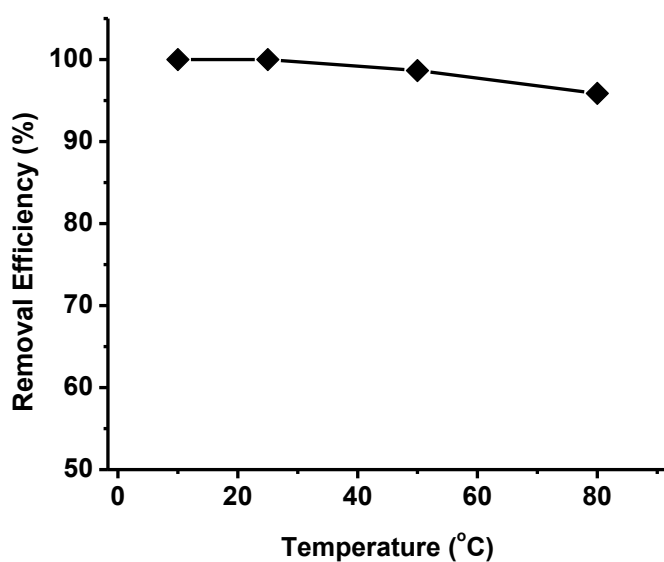


Figure S10. Temperature dependency plot for mercury adsorption using 5 ppm Hg(II) solution after 2h.

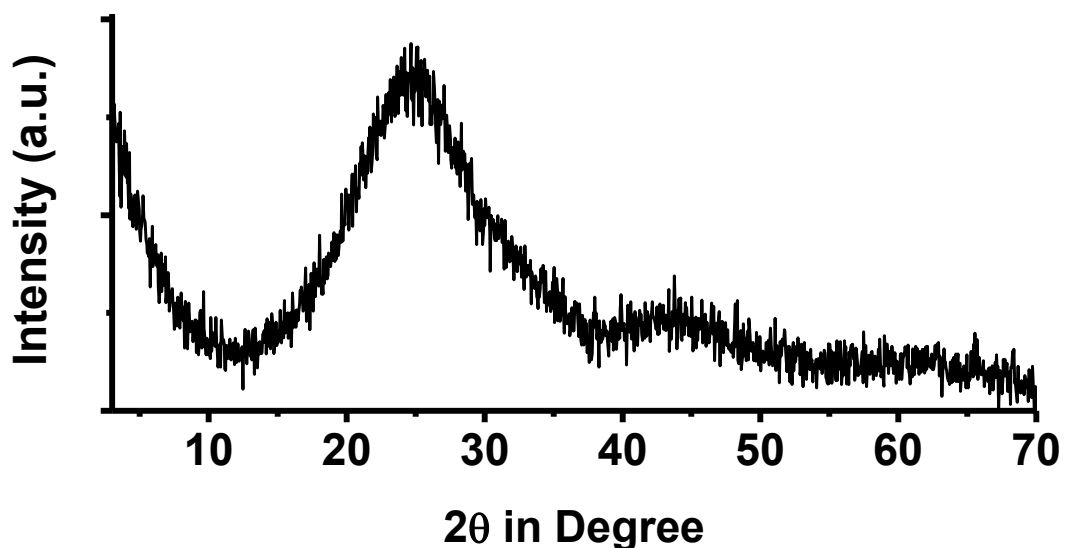


Figure S11. Wide angle X-ray diffraction pattern of recycled SCTN-1.

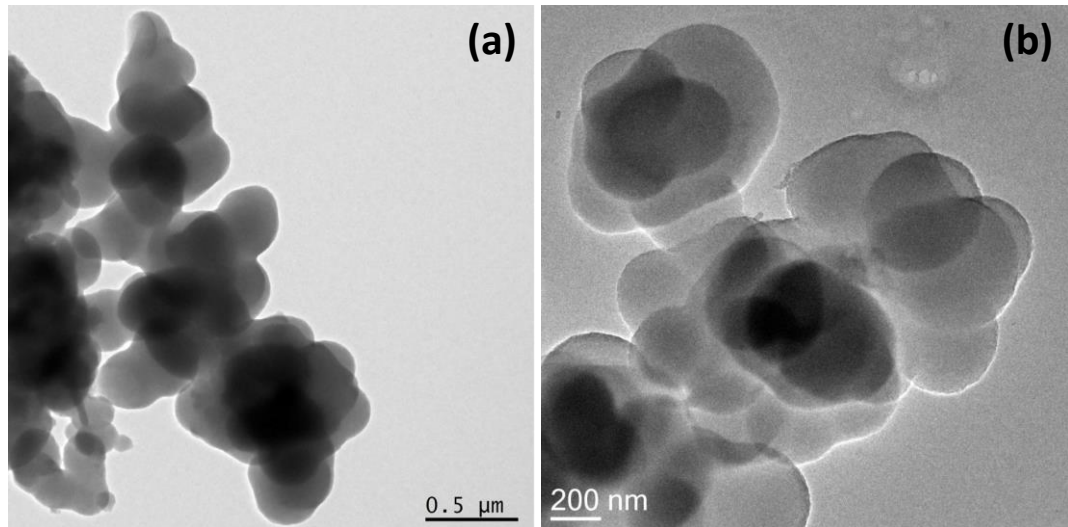


Figure S12. TEM images of reused SCTN-1.

Reference

1. M. J. Frisch, G. W. T., H. B. Schlegel, G. E. Scuseria, M. A. Robb, J. R. Cheeseman, G. Scalmani, V. Barone, G. A. Petersson, H. Nakatsuji, X. Li, M. Caricato, A. V. Marenich, J. Bloino, B. G. Janesko, R. Gomperts, B. Mennucci, H. P. Hratchian, J. V. Ortiz, A. F. Izmaylov, J. L. Sonnenberg, D. Williams Young, ; F. Ding, F. L., F. Egidi, J. Goings, B. Peng, A. Petrone, T. Henderson, D. Ranasinghe, V. G. Zakrzewski, J. Gao, N. Rega, G. Zheng, W. Liang, M. Hada, M. Ehara, K. Toyota, R. Fukuda, J. Hasegawa, M. Ishida, T. Nakajima, Y. Honda, O. Kitao, H. Nakai, T. Vreven, K. Throssell, J. A. Montgomery, Jr., J. E. Peralta, F. Ogliaro, M. J. Bearpark, J. J. Heyd, E. N. Brothers, K. N. Kudin, V. N. Staroverov, T. A. Keith, R. Kobayashi, J. Normand, K. Raghavachari, A. P. Rendell, J. C. Burant, S. S. Iyengar, J. Tomasi, M. Cossi, J. M. Millam, M. Klene, C. Adamo, R. Cammi, J. W. Ochterski, R. L. Martin, K. Morokuma, O. Farkas, J. B. Foresman, and D. J. Fox, Gaussian 16, Revision A.03. *Gaussian, Inc.*, Wallingford CT 2016.
2. Yamanou, K.; Tatamitani, Y.; Ogata, T., Three Intermolecular Bonds Form a Weak but Rigid Complex: O(CH₃)₂···N₂O. *J. Phys. Chem. A* **2009**, *113* (15), 3476-3480.
3. Solimannejad, M.; Pejov, L., Computational Investigation of the Weakly-Bound Dimers HOX···SO₃ (X = F, Cl, Br). *J. Phys. Chem. A* **2005**, *109* (5), 825-831.
4. Bu, Y.; Cao, Z., Structures and Bonding Character of Ge···CO Weakly Bonding Complexes. *J. Phys. Chem. B* **2002**, *106* (7), 1613-1621.
5. Wesolowski, T. A.; Parisel, O.; Ellinger, Y.; Weber, J., Comparative Study of Benzene···X (X = O₂, N₂, CO) Complexes Using Density Functional Theory: The Importance of an Accurate Exchange–Correlation Energy Density at High Reduced Density Gradients. *J. Phys. Chem. A* **1997**, *101* (42), 7818-7825.
6. Nowek, A.; Leszczyński, J., Molecular Structure of the GeH₂···OH₂ Complex. *J. Phys. Chem. A* **1997**, *101* (20), 3784-3788.

7. Ching, J. C.; Schlemper, E. O., Slightly constrained O---O hydrogen bond. Crystal structure of a tetradentate .alpha.-amine oxime complex of nickel(II). *Inorg. Chem.* **1975**, *14* (10), 2470-2474.
8. Bader, R. W.; Matta, C., Atoms in molecules as non-overlapping, bounded, space-filling open quantum systems. *Found Chem* **2013**, *15* (3), 253-276.
9. Bader, R. F. W., The density in density functional theory. *Comp. Theor. Chem.* **2010**, *943* (1-3), 2-18.
10. Bader, R. F. W., Bond Paths Are Not Chemical Bonds. *J. Phys. Chem. A* **2009**, *113* (38), 10391-10396.
11. Matta, C. F.; Bader, R. F. W., An Experimentalist's Reply to "What Is an Atom in a Molecule?". *J. Phys. Chem. A* **2006**, *110* (19), 6365-6371.
12. Bader, R. F. W., Comment on the Comparative Use of the Electron Density and Its Laplacian. *Chem. Eur. J.* **2006**, *12* (30), 7769-7772.
13. Bader, R. F. W., Comment on Revisiting the variational nature of the quantum theory of atoms in molecules. *Chem. Phys. Lett.* **2006**, *426* (1-3), 226-228.
14. Cortés-Guzmán, F.; Bader, R. F. W., Complementarity of QTAIM and MO theory in the study of bonding in donor-acceptor complexes. *Coord. Chem. Rev.* **2005**, *249* (5-6), 633-662.
15. Bader, R. F. W.; Gillespie, R. J.; Martín, F., Core distortions in metal atoms and the use of effective core potentials. *Chem. Phys. Lett.* **1998**, *290* (4-6), 488-494.
16. Bone, R. G. A.; Bader, R. F. W., Identifying and Analyzing Intermolecular Bonding Interactions in van der Waals Molecules†. *J. Phys. Chem.* **1996**, *100* (26), 10892-10911.
17. Bader, R. F. W., Molecular fragments or chemical bonds. *Acc. Chem. Res.* **1975**, *8* (1), 34-40.